ACS APPLIED MATERIALS & INTERFACES

Research Article

www.acsami.org

Nitrogen Self-Doped Porous Carbon from Surplus Sludge as Metal-Free Electrocatalysts for Oxygen Reduction Reactions

Kai Zhou,[†] Weijia Zhou,*[,†] Xiaojun Liu,[†] Yan Wang,[†,‡,§] Jinquan Wan,[†,‡,§] and Shaowei Chen*[,†,∥]

[†]New Energy Research Institute, College of Environment and Energy, South China University of Technology, Guangzhou Higher Education Mega Center, Guangzhou, Guangdong 510006, China

[‡]State Key Lab of Pulp and Paper Engineering, South China University of Technology, Guangzhou, Guangdong 510640, China

[§]Key Lab of Pollution Control and Ecosystem Restoration in Industrial Clusters, Ministry of Education, Guangzhou, Guangdong 510006, China

[∥]Department of Chemistry and Biochemistry, University of California, 1156 High Street, Santa Cruz, California 95064, United States

Supporting Information

ABSTRACT: Nitrogen self-doped porous carbon was prepared by calcination treatment of surplus sludge, a toxic byproduct from microbial wastewater treatments, and exhibited a mesoporous structure, as manifested in scanning and transmission electron microscopic measurements. Nitrogen adsorption/desorption studies showed that the porous carbon featured a BET surface area as high as 310.8 m^2/g and a rather broad range of pore size from 5 to 80 nm. X-ray photoelectron spectroscopic studies confirmed the incorporation of nitrogen into the graphitic matrix forming pyridinic and pyrrolic moieties. Interestingly, the obtained porous carbon exhibited apparent electrocatalytic activity in oxygen reduction in alkaline media, with the optimal temperatures identified within the range of 600 to 800 °C, where the number of electron transfers involved in oxygen reduction was estimated to be 3.5 to 3.7 and the performance was rather comparable to leading literature results as a consequence of deliberate engineering of the graphitic matrix by nitrogen doping.

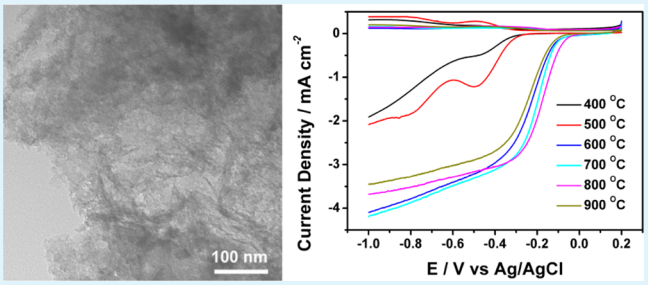

KEYWORDS: *carbonization, carbon nanosheet, nitrogen adsorption/desorption, methanol crossover, CO poisoning*

INTRODUCTION

Fuel cells represent a unique technology that offers clean and sustainable energy with minimal adverse impacts on the environment. Yet there remain several critical challenges that hamper the performance of fuel cells. One of these is the development of efficient electrocatalysts for oxygen reduction reactions (ORR) at the cathode, and platinum-based nanoparticles have been recognized as the leading catalysts of choice for ORR.[1−5] However, the high cost, scarcity, and poor durability of Pt-based noble metals severely limit their widespread applications in ORR. Thus, exploring low-cost, non-noble metal or even metal-free catalysts for ORR has been attracting extensive interest.[6−13] Among these, recently metal-free carbon nanomaterials doped with nitrogen, boron, sulfur, and phosphorus have been found to exhibit striking electrocatalytic activity for ORR.[13−21] For example, Wei et al.[22] reported that nitrogen-doped carbon nanosheets with size-defined mesopores behaved as highly efficient metal-free ORR catalysts. Controlled mesoporous structures and nitrogen-doping exerts an essential influence on the electrocatalytic performance in both alkaline and acidic media for ORR electrocatalysis.

In the present study, we prepare a new type of nonmetal catalysts for ORR by calcination treatment of surplus sludge obtained from microbial wastewater treatments. As a leading method in wastewater treatment, microbial cells are used to adsorb and transform organic pollutants and metal ions (such as Mn^{4+}, Co^{3+}, and Cu^{2+}) in wastewater,[23,24] and produce abundant surplus sludge as byproducts. Yet, how to deal with the polluting surplus sludge is a difficult issue in environmental research.[25,26] As surplus sludge is typically rich in carbon and nitrogen (from microbial cells) and metals (from wastewater), important components known to exhibit electrocatalytic activity in ORR,[27−29] an immediate question arises: Can these materials be used to prepare valuable and high-performance electrocatalysts? Note that studies of such a waste-to-wealth scheme with surplus sludge have been scarce.[30,31] This is the primary motivation of the present study.

Herein, surplus sludge was used as carbon and nitrogen sources to synthesize nitrogen self-doped porous carbon as metal-free electrocatalysts for ORR. The sludge was obtained

Received: April 11, 2014
Accepted: August 19, 2014
Published: August 19, 2014

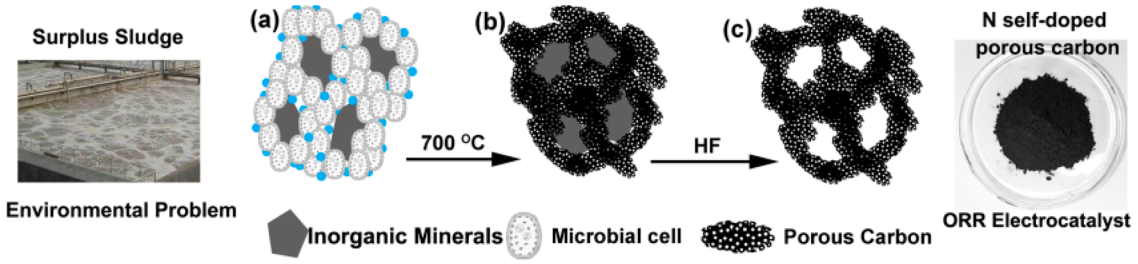

Figure 1. Schematic of the synthesis of porous carbon from surplus sludge.

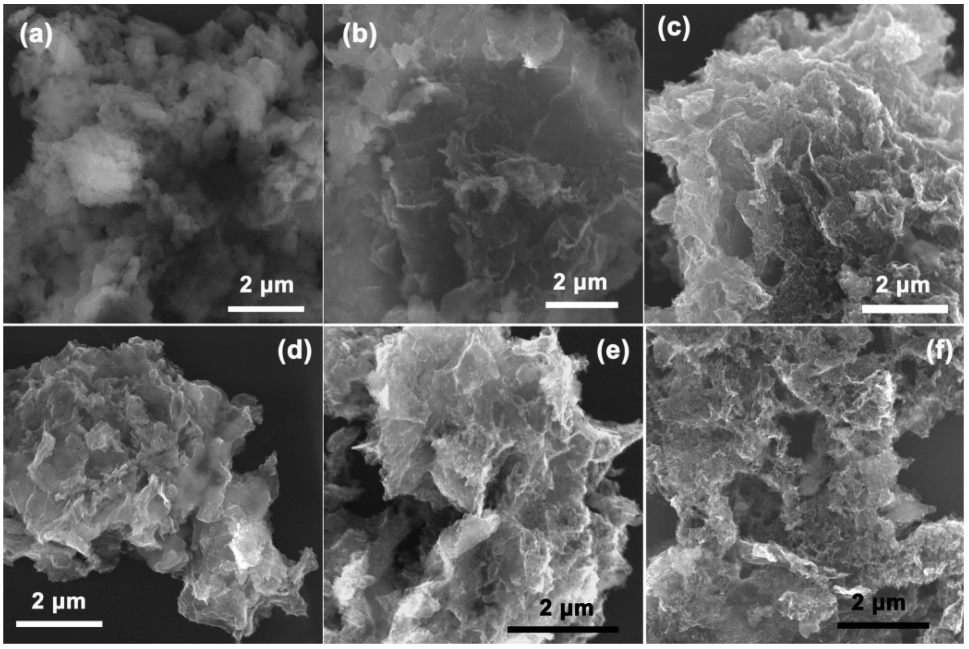

Figure 2. SEM images of porous carbon prepared at different calcination temperatures: (a) 400 °C, (b) 500 °C, (c) 600 °C, (d) 700 °C, (e) 800 °C, and (f) 900 °C. Scale bars are all 2 μm.

from a local wastewater treatment plant, which was rich in microbial cells and inorganic minerals but no heavy metal ions. N-doped porous carbon materials were produced by simple carbonization of the sludge under an inert atmosphere at controlled temperatures ranging from 400 to 900 °C and exhibited apparent electrocatalytic activity for ORR, excellent durability, and tolerance toward methanol crossover and CO poisoning, in comparison to leading commercial Pt/C catalysts.

EXPERIMENTAL SECTION

Materials. Hydrofluoric acid (HF) were purchased from Sinopharm Chemical Reagents Co., Ltd. Water was supplied with a Barnstead Nanopure Water System (18.3 MΩ·cm). Surplus sludge was obtained from the secondary sedimentation tank of the Lijiao Wastewater Treatment Plant, Guangzhou, China. The sludge was dried in an oven at 105 °C, further ground, and sieved to 100 mesh.

Synthesis of Nitrogen Self-Doped Porous Carbon. To synthesize nitrogen self-doped porous carbon, dried sludge was heated in a tubular furnace at controlled temperatures (400−900 °C) for 2 h in a N_2 atmosphere, and the gases produced during the heating process were filtered by a KOH aqueous solution before being released into the ventilation system. The resulting carbonized powders were washed with HF (40%), and then washing by Nanopure water until pH = 7. Finally, the nitrogen self-doped porous carbon sample was dried in an oven at 60 °C for 12 h.

Characterization. The morphologies and structures of the samples were examined with a Hitachi S-4800 field emission scanning electron microscope (FESEM) and a JEOL JEM-2100 transmission electron microscope (TEM) at an acceleration voltage of 200 kV. The BET surface area and pore size distribution were characterized with a Micromeritics ASAP 2010 by nitrogen adsorption at 77 K and the Barrett−Joyner−Halenda (BJH) method. X-ray photoelectron spectroscopy (XPS) studies were performed with an ESCALAB 250 instrument.

Electrochemistry. Voltammetric studies were carried out in a conventional three-electrode cell with a CHI 660E Electrochemical Workstation (CH Instruments, China). The working electrode was a rotating (gold) ring-(glassy carbon) disk electrode (RRDE, disk diameter 4.57 mm, with a collection efficiency (N) of 37%). A Ag/AgCl electrode (saturated KCl) and a Pt electrode were used as the reference and counter electrodes, respectively. To prepare electrocatalysts on the glassy carbon electrode surface, 4 mg of the N-doped porous carbon was dispersed by sonication into 1 mL of a mixture of ethanol and water (v:v 1:4), into which was then added 40 μL of Nafion (5%). Ten microliters of the resulting catalyst ink was drop-cast onto the surface of the glassy carbon electrode with a Hamilton microliter syringe. The electrode was dried at ambient temperature for 12 h prior to immersion into the electrochemical cell for data acquisition. For comparison, a calculated amount of commercial Pt/C (20 wt %) catalysts (ca. 40 μg) was loaded onto the electrode surface in a similar fashion.

RESULTS AND DISCUSSION

The synthetic procedure for N-doped porous carbon by carbonization of surplus sludge is shown in Figure 1. The

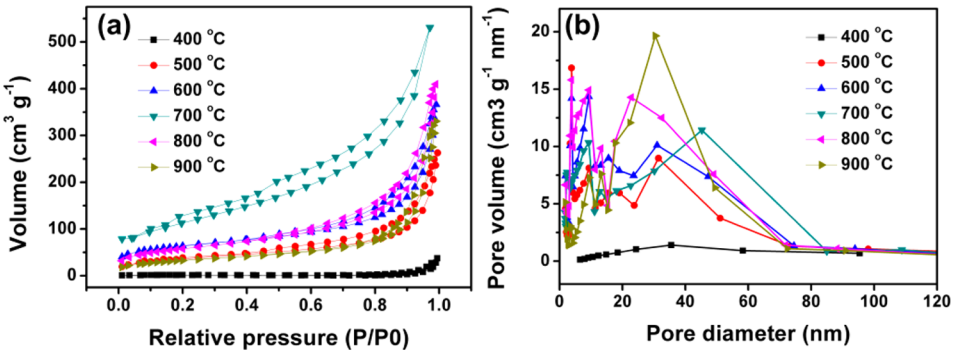

Figure 3. (a) Nitrogen adsorption/desorption isotherms and (b) pore size distribution of porous carbon synthesized at different calcination temperatures.

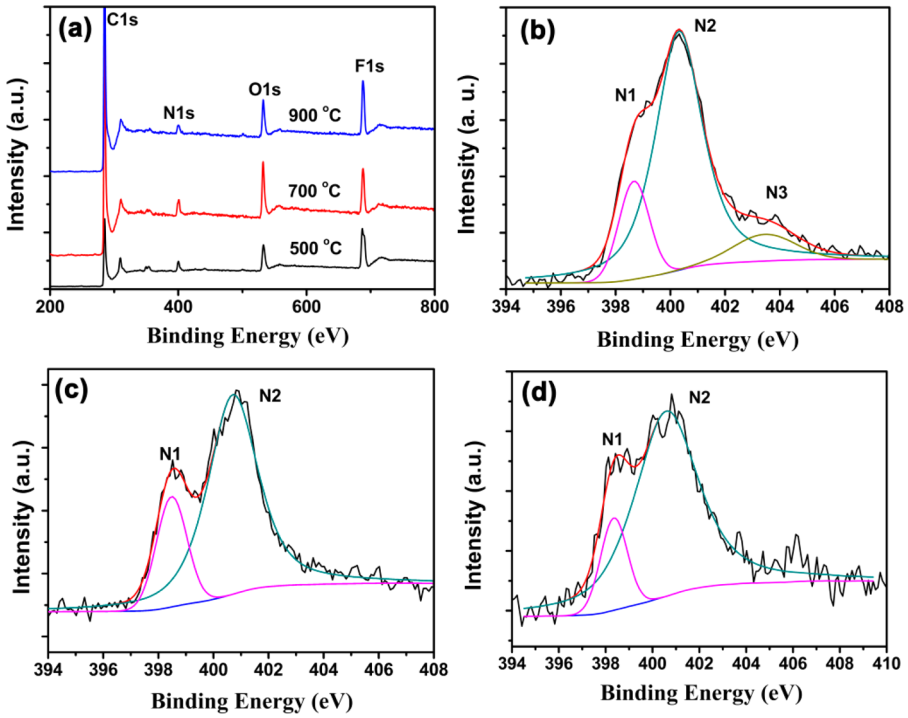

Figure 4. (a) XPS survey spectra of nitrogen self-doped porous carbon prepared from carbonization of surplus sludge at different calcination temperatures and high-resolution scan of the N 1s electrons: (b) 500 °C, (c) 700 °C, and (d) 900 °C. In panels (b), (c), and (d), black curve is the experimental raw data, blue curve is the baseline, magenta and green curves are deconvolution fits, and red curve is the sum of the fits.

surplus sludge used herein is composed mostly of inorganic minerals and organic materials (Supporting Information (SI) Table S1). Note that surplus sludge typically entails an inorganic skeleton made up mostly of inorganic mineral particles on which microbial cells are adsorbed, as depicted in panel (a). The mixture was then calcined at elevated temperatures for 2 h in an inert atmosphere. After the heat treatment, the microbial cells and organic contaminants were carbonized, leading to the formation of a porous carbon matrix supported on the inorganic scaffolds (panel (b)). Then, HF was used to remove the inorganic mineral particles forming a mesoporous structure with porous carbon stacked together (panel (c)), as manifested by a marked increase of the specific surface area and pore size distribution (SI Figure S1). Such a strategy not only helps solve the problems of environmental pollution by surplus sludge but may also be exploited for the production of effective ORR electrode materials (vide infra).

The effects of calcination temperature on the morphologies and specific surface area of obtained porous carbon were then studied. The corresponding SEM images and BET surface area results are shown in Figure 2 and Figure 3, respectively. From Figure 2, it can be seen that except for the samples synthesized at low temperatures (400 and 500 °C), the samples obtained at higher temperatures (600 to 900 °C) exhibited a porous structure with a rough flaky surface morphology. The porous characteristics can be further resolved in TEM measurements (SI Figure S2), where one can see that the porous carbon nanosheets are stacked and folded together forming a worm-like mesoporous structure.

The specific surface area and pore size distribution of the N-doped porous carbon were then quantified by nitrogen adsorption/desorption studies. From Figure 3, it can be seen that the porous carbon all exhibited type IV nitrogen adsorption/desorption isotherms with a clear H_2-type hysteresis loop, consistent with the formation of a mesoporous network (Figure 3a). The specific surface areas are estimated to be 4.51 m^2/g, 127.9 m^2/g, 216.3m^2/g, 310.8 m^2/g, 204 m^2/g, and 116.9 m^2/g for the porous carbon prepared at 400 °C, 500

dx.doi.org/10.1021/am502215t | ACS Appl. Mater. Interfaces 2014, 6, 14911−14918

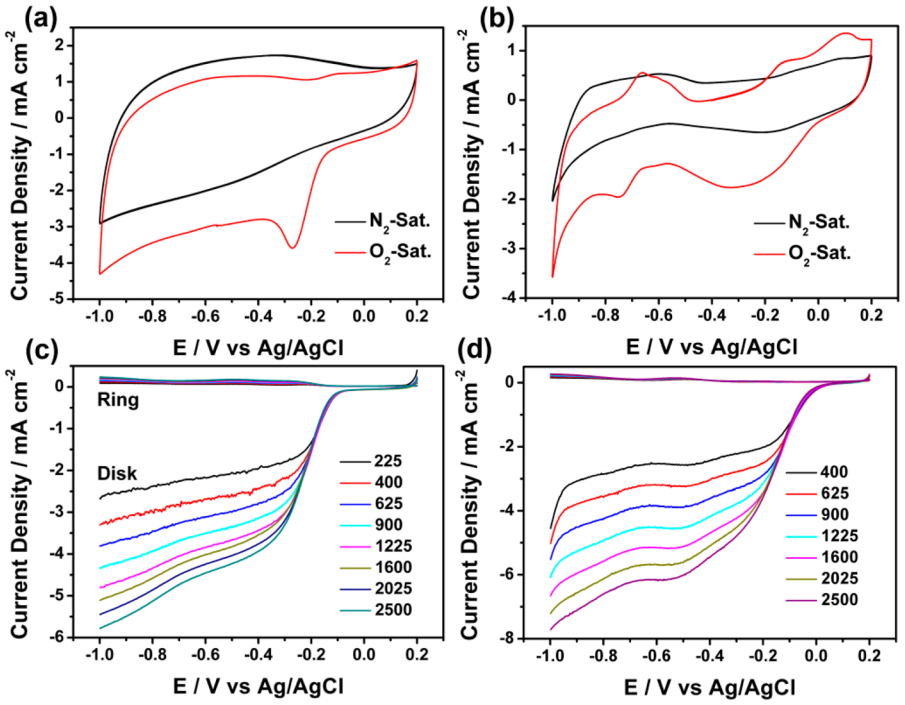

Figure 5. Cyclic voltammograms of (a) nitrogen self-doped porous carbon prepared at 700 °C and (b) 20 wt % Pt/C at a potential scan rate of 100 mV/s in an oxygen- or nitrogen-saturated 0.1 M KOH solution. RRDE voltammograms of (c) nitrogen self-doped porous carbon prepared at 700 °C and (d) 20 wt % Pt/C in an oxygen-saturated 0.1 M KOH solution at different rotation rates which are specified in the figure legends in rpm. Ring potential was set at +0.50 V. The electrode geometrical surface area (16.4 mm^2) was used to calculate the current density.

°C, 600 °C, 700 °C, 800 °C, and 900 °C, respectively. That is, among the series, the BET surface area was the lowest for the 400 °C sample, likely due to insufficient carbonization of the surplus sludge, but increased to the highest value of 310.8 m^2/g for the 700 °C sample, then decreased to 116.9 m^2/g for samples prepared at 900 °C where collapse of the porous structures likely occurred. Furthermore, the porous carbon exhibited a rather broad pore size range from 5 to 80 nm (Figure 3b), suggesting the formation of a disordered worm-like mesoporous structure, which is consistent with results from TEM measurements (SI Figure S2).

The elemental compositions of the N-doped porous carbon were then investigated by XPS measurements. The survey spectra in Figure 4a clearly show the presence of carbon, nitrogen, oxygen, and fluorine elements within the samples (no metal elements can be identified), where the F element most likely came from residual HF in the washing process. The absence of Ca, Al, and Si that were found in the original sludge indicates that HF washing effectively removed the inorganic minerals from the samples (SI Figure S3). High-resolution scans of the N 1s electrons for samples prepared at different calcination temperatures, (b) 500 °C, (c) 700 °C, and (d) 900 °C, all show two peaks at 398.5 and 400.3 eV, which are consistent with pyridinic (N1) and pyrrolic (N2) nitrogen, respectively, indicating successful incorporation of N into the graphitic matrix.[14,32] Note that these are known to be the active sites for ORR.[21] For N-doped porous carbon prepared at 500 °C (panel (b)), an additional peak emerged at 403.5 eV which is assigned to quaternary nitrogen (N3) that is known to be ORR-inactive.[21] Furthermore, based on the integrated peak areas of the C 1s and N 1s electrons, the fraction of nitrogen dopants was estimated to be 11.9 at. % (500 °C, panel (b)), 6.5 at. % (700 °C, panel (c)), and 4.3 at. % (900 °C, panel (d)), respectively, signifying a decrease of the nitrogen doping level with increasing calcination temperature.

Interestingly, the N-doped porous carbon exhibited apparent electrocatalytic activity for ORR in alkaline media, as manifested in Figure 5, with commercial Pt/C (20 wt %) catalysts as the benchmark materials. From the cyclic voltammograms in panels (a) and (b), one can see that for both samples, the voltammetric profiles in N_2-saturated 0.1 M KOH were largely featureless (black curves); yet when the electrolyte solution was saturated with oxygen, apparent cathodic currents (red curves) started to emerge when the electrode potentials were swept cathodically, suggesting electrocatalytic reduction of oxygen by both N-doped porous carbon and Pt/C.

Consistent results were obtained in RRDE measurements. Figure 5c depicts the RRDE voltammograms of the nitrogen self-doped porous carbon prepared at 700 °C in an oxygen-saturated 0.1 M KOH solution at different rotation rates. It can be seen that nonzero cathodic currents started to emerge at the electrode potential of about −0.04 V, increased drastically with increasingly negative electrode potentials, and reached a quasi-plateau at potentials more negative than ca. −0.30 V. This signifies effective electrocatalytic reduction of oxygen by the porous carbon. Interestingly the performance was rather comparable to that of leading commercial Pt/C 20 wt % catalysts at similar mass loadings, which was shown in panel (d). For instance, at 900 rpm, the current density was about 3.48 mA cm^{-2} for the porous carbon catalyst, which was only slightly lower than that observed with Pt/C (3.85 mA cm^{-2}). In addition, one can see that at both catalysts, the ring currents were at least an order of magnitude lower than the disk currents, indicating the production of minimal amounts of peroxide intermediates. In fact, the number of electron transfer (n) involved in oxygen reduction, as estimated by $n = 4I_D/(I_D +$

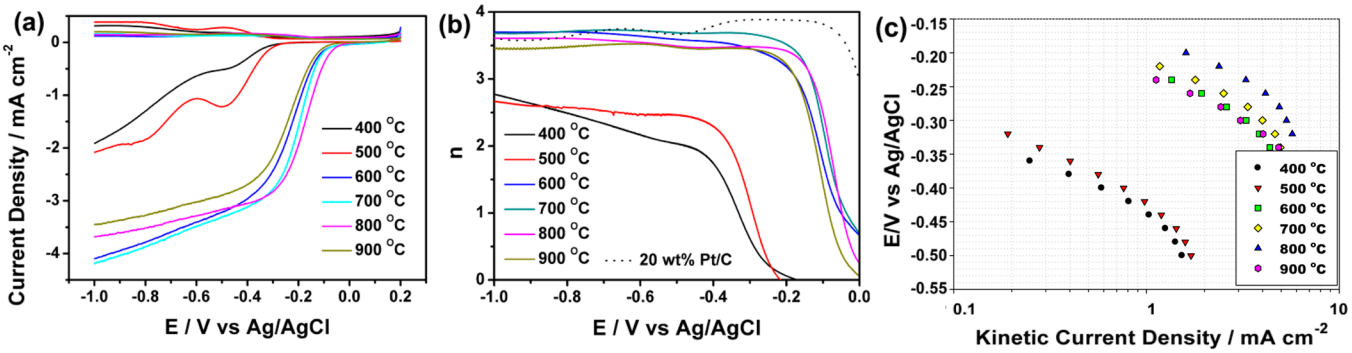

Figure 6. (a) RRDE voltammograms of the porous carbon samples prepared at different calcination temperatures (specified in figure legends) in an O_2-saturated 0.1 M KOH solution at a rotation rate of 900 rpm. The electrode geometrical surface area (16.4 mm^2) was used to calculate the current density. (b) Corresponding number of electron transfers (n) involved in ORR at varied electrode potentials. (c) Tafel plot of the porous carbon samples obtained at different calcination temperatures in oxygen reduction.

Table 1. Summary of ORR Performance of N-Doped Porous Carbon

	nitrogen self-doped porous carbon					
Calcination temperature (°C)	400	500	600	700	800	900
Onset potential (V vs Ag/AgCl)	−0.26	−0.24	−0.06	−0.04	−0.02	−0.05
Tafel slope (mV/dec)	127	132	154	130	128	134
Current density (mA cm^{-2}) at −0.6 V and 900 rpm	−0.64	−1.07	−3.40	−3.48	−3.29	−3.02

I_R/N), where I_D is the disk current, I_R is the ring current, and N is the collection efficiency (0.37), shows that $n \approx 3.7$ within the range of −0.3 to −1.0 V for the porous carbon catalysts and 3.7−3.9 for commercial Pt/C (Figure 6). This suggests that OH^- was the dominant product of oxygen reduction, $O_2 + 2H_2O + 4e \rightarrow 4OH^-$, with the yield of H_2O_2 from ORR only 14% to 22% (SI Figure S4), Nevertheless, one may notice that the onset potential for ORR was markedly more negative for the porous carbon (−0.04 V) than for Pt/C (+0.08 V), signifying a subpar performance of the porous carbon as compared to commercial Pt/C.

The effects of carbonization temperature on the ORR performance of the N-doped porous carbon were then examined by voltammetric measurements. As depicted in Figure 6a, RRDE voltammetric measurements showed apparent ORR activity for all samples prepared by calcination treatment within the temperature range of 400 to 900 °C, with nonzero cathodic currents at sufficiently negative electrode potentials. However, clear discrepancy of the ORR activity can be seen among the samples. For instance, the cathodic current density at −0.60 V increased in the order of 400 °C (−0.64 mA cm^{-2}) < 500 °C (−1.07 mA cm^{-2}) < 900 °C (−3.02 mA cm^{-2}) < 800 °C (−3.29 mA cm^{-2}) < 600 °C (−3.40 mA cm^{-2}) < 700 °C (−3.48 mA cm^{-2}). That is, the samples prepared at 700 °C exhibited the best performance among the series (Table 1). The variation of the ORR activity can also be manifested by the number of electron transfers involved in ORR (n), as depicted in panel (b). For instance, the n value at −0.60 V increases in the order of 2.2 (400 °C) < 2.5 (500 °C) < 3.5 (900 °C) ≈ 3.5 (800 °C) < 3.6 (600 °C) < 3.7 (700 °C), with the 700 °C sample again standing out as the best catalyst. In addition, the onset potential for ORR was found to vary with the porous carbon samples as well, −0.26 V (400 °C), −0.24 V (500 °C), −0.06 V (600 °C), −0.04 V (700 °C), −0.02 V (800 °C), and −0.05 V (900 °C). Taken together, these results (Table 1) suggest that 600 to 800 °C appears to be the optimal range of calcination temperature in the preparation of porous carbon for ORR electrocatalysis.

The electron-transfer kinetics involved were then quantified by Koutecky−Levich analysis (eq 1a),[33] as the disk currents (I_D) might include both kinetic (I_k) and diffusion (I_d)-controlled contributions

$$\frac{1}{I_D} = \frac{1}{I_k} + \frac{1}{I_d} = \frac{1}{I_k} + \frac{1}{B\omega^{1/2}} \quad (1a)$$

$$B = 0.62nFAC_O D_O^{2/3} \nu_0^{-1/6} \quad (1b)$$

$$I_k = nAFkC_0 \quad (1c)$$

where F is the Faradaic constant (96500 C/mol), D_O the diffusion coefficient of O_2 in solution (1.93×10^{-5} cm^2/s), ν the kinematic viscosity of the solution (9.87×10^{-3} cm^2/s), C_O the oxygen concentration in O_2-saturated solutions (1.18 mM), ω the electrode rotation rate, k the electron-transfer rate constant, and A the geometric surface area of the electrode. SI Figure S5 depicts the Koutecky−Levich plots (I_D^{-1} vs $\omega^{-1/2}$) of all porous carbon samples within the respective kinetically controlled region. First, one can see that all experimental data exhibited good linearity, and the slopes were rather consistent with each porous carbon sample. This indicates that the oxygen reduction proceeded at the porous carbon catalysts as a first-order reaction with respect to dissolved oxygen. In addition, from the linear regressions in SI Figure S5, the kinetic currents (I_k) could also be quantified from the y-axis intercepts (eq 1c). This is manifested in the Tafel plot of Figure 6c. It can be seen that at the same electrode potentials, the kinetic current density exhibited a clear variation with the porous carbon samples. For instance, at −0.32 V, J_k increases in the order of 0.19 mA cm^{-2} (500 °C) < 3.84 mA cm^{-2} (600 °C) < 4.02 mA cm^{-2} (900 °C) < 4.64 mA cm^{-2} (700 °C) < 5.70 mA cm^{-2} (800 °C)—note that the ORR activity of the 400 °C sample at this potential was too low to be detected. These results again signify that calcination temperatures at 600 °C and higher are preferred to produce effective electrocatalysts for ORR. In addition, linear regressions of the Tafel plots in the low overpotential regions yield a slope between 120 and 150 mV dec^{-1} for the series of

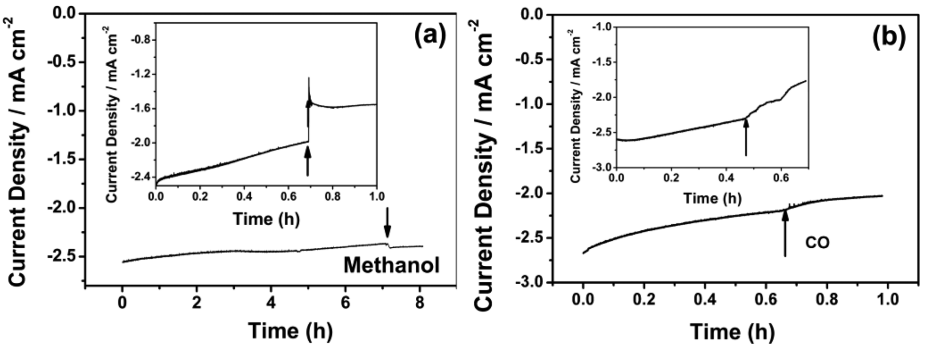

Figure 7. Chronoamperometric profiles of N-doped porous carbon (700 °C) at −0.4 V at a rotation rate of 900 rpm before and after the injection of (a) 5 mL of methanol and (b) CO. Insets to (a) and (b) are the corresponding chronoamperometric profiles with 20 wt % Pt/C, respectively.

nitrogen self-doped porous carbon (Table 1). Note that for oxygen electroreduction at nanoparticle catalyst surfaces, the Tafel slopes are typically found at 60 mV dec^{-1} or 120 mV dec^{-1}, where the former corresponds to a pseudo two-electron reaction as the rate-determining step, and in the latter, the rate-determining step, is presumed to be the first-electron reduction of oxygen.[34] Therefore, it is likely that in the low overpotential regime oxygen reduction on the N-doped porous carbon surface was largely limited by the first-electron reduction of oxygen.[13−21]

Importantly, the N-doped porous carbon also showed excellent durability and tolerance toward methanol crossover and CO poisoning, as depicted in Figure 7. We used the voltammetric currents at −0.40 V as the illustrating example. Chronoamperometric measurements showed that the cathodic current decreased by less than 10% for continuous operation up to 7 h (panel (a)); and when methanol or CO was injected into the electrolyte, the cathodic currents remained virtually unchanged. In contrast, commercial Pt/C (20 wt %) catalysts can be easily poisoned by methanol and CO, leading to a sharp diminishment of the voltammetric currents (Figure 7 insets).

The aforementioned results reveal the high ORR electrocatalytic activity, stability, and tolerance toward methanol and CO poisoning of N-doped porous carbon. The performance is rather comparable to or even better than typical literature results of similar systems, such as phosphorus-doped graphite layers (onset potential −0.10 V vs Ag/AgCl, n ≈ 3),[18] and nitrogen-doped graphene (onset potential −0.20 V vs Ag/AgCl, n = 3.6 to 4),[32] nitrogen-doped porous carbon nanopolyhedra (onset potential −0.02 V vs Ag/AgCl, n = 3.6 to 3.8),[19] and nitrogen and phosphorus dual-doped hierarchical porous carbon foams (onset potential −0.03 V vs Ag/AgCl, n = 3.0 to 4.0).[20] A major advantage of the strategy developed in this work is converting toxic chemical wastes into functional and valuable materials, which not only helps solve the problem of environmental pollution by surplus sludge but also can be exploited for the production of a new type of effective ORR electrode materials. The remarkable ORR performance observed herein with the nitrogen self-doped porous carbon may be attributed to the following factors. First, the carbon obtained from surplus sludge exhibits a porous structure with a high surface area and a rather broad range of pore size (Figures 3 and S1 (in SI)), which facilitate ready accessibility to electrolytes and O_2 and hence oxygen reduction. In fact, for the porous carbons prepared under identical conditions but without HF acid washing, the ORR activity was markedly lower than that with HF acid washing, within the context of onset potential, n values, and current density (SI Figure S6), which also signifies minimal contribution of the inorganic oxides to the observed electrocatalytic activity in ORR. Second, nitrogen doping within the graphitic matrix led to the formation of active sites for oxygen adsorption and eventual reduction, as carbon π electrons might be activated by conjugation with the pyridinic and pyrrolic nitrogen dopants.[15,32] In the present study, nitrogen dopants originated mainly from amino acids in microbial cells in the surplus sludge.[35,36]

CONCLUSION

In summary, N-doped porous carbon was readily obtained by a simple yet effective procedure based on calcination treatments of surplus sludge, a toxic byproduct from wastewater treatment, and exhibited apparent electrocatalytic activity as a metal-free catalyst for oxygen reduction, with the optimal range of temperature identified within 600 to 800 °C. The obtained N-doped carbon (e.g., 700 °C) featured a mesoporous structure with a BET surface area as high as 310.8 m^2/g and a rather broad range of pore size from 5 to 80 nm. Significantly, the electrocatalytic performance was found to be rather comparable to leading literature results of similar systems, within the context of onset potential, number of electron transfer, as well as tolerance against methanol and CO poisoning.

ASSOCIATED CONTENT

Supporting Information

Representative TEM micrograph, specific surface area and pore volume of the samples prepared at 700 °C but without HF acid washing, and additional voltammetric data of ORR electrocatalysis. This material is available free of charge via the Internet at http://pubs.acs.org.

AUTHOR INFORMATION

Corresponding Authors

*E-mail: eszhouwj@scut.edu.cn.

*E-mail: shaowei@ucsc.edu.

Notes

The authors declare no competing financial interest.

ACKNOWLEDGMENTS

This work was supported by the Recruitment Program of Global Experts, the PhD Start-up Funds of the Natural Science Foundation of Guangdong Province (x2hjB6130130), Zhujiang New Stars of Science & Technology (x2hjB2140700), the Fundamental Research Funds for Central Universities (x2hjD2131690), and the National Natural Science Foundation

of China (No. 31200458). S.W.C. also acknowledges support from the US National Science Foundation (CHE−1265635).

REFERENCES

(1) Xia, B. Y.; Ng, W. T.; Wu, H. B.; Wang, X.; Lou, X. W. Self-Supported Interconnected Pt Nanoassemblies as Highly Stable Electrocatalysts for Low-Temperature Fuel Cells. *Angew. Chem., Int. Ed* **2012**, *51*, 7213−7216.

(2) Zhang, S.; Guo, S. J.; Zhu, H. Y.; Su, D.; Sun, S. H. Structure-Induced Enhancement in Electrooxidation of Trimetallic FePtAu Nanoparticles. *J. Am. Chem. Soc.* **2012**, *134*, 5060−5063.

(3) Zhou, Z. Y.; Kang, X. W.; Song, Y.; Chen, S. W. Enhancement of the Electrocatalytic activity of Pt Nanoparticles in Oxygen Reduction by Chlorophenyl Functionalization. *Chem. Commun.* **2012**, *48*, 3391−3393.

(4) Lee, E. P.; Peng, Z. M.; Chen, W.; Chen, S. W.; Yang, H.; Xia, Y. N. Electrocatalytic Properties of Pt Nanowires Supported on Pt and W Gauzes. *ACS Nano* **2008**, *2*, 2167−2173.

(5) Mayrhofer, K. J. J.; Strmcnik, D.; Blizanac, B. B.; Stamenkovic, V.; Arenz, M.; Markovic, N. M. Measurement of Oxygen Reduction Activities via the Rotating Disc Electrode Method: From Pt Model Surfaces to Carbon-Supported High Surface Area Catalysts. *Electrochim. Acta* **2008**, *53*, 3181−3188.

(6) Zhao, D.; Shui, J.-L.; Grabstanowicz, L. R.; Chen, C.; Commet, S. M.; Xu, T.; Lu, J.; Liu, D.-J. Electrocatalysts: Highly Efficient Non-Precious Metal Electrocatalysts Prepared from One-Pot Synthesized Zeolitic Imidazolate Frameworks. *Adv. Mater.* **2014**, *26*, 1092−1092.

(7) Wu, Z.-S.; Chen, L.; Liu, J.; Parvez, K.; Liang, H.; Shu, J.; Sachdev, H.; Graf, R.; Feng, X.; Müllen, K. High-Performance Electrocatalysts for Oxygen Reduction Derived from Cobalt Porphyrin-Based Conjugated Mesoporous Polymers. *Adv. Mater.* **2014**, *26*, 1450−1455.

(8) Deng, D.; Yu, L.; Chen, X.; Wang, G.; Jin, L.; Pan, X.; Deng, J.; Sun, G.; Bao, X. Iron Encapsulated within Pod-like Carbon Nanotubes for Oxygen Reduction Reaction. *Angew. Chem. Int. Ed* **2013**, *52*, 371−375.

(9) Liang, Y. Y.; Li, Y. G.; Wang, H. L.; Zhou, J. G.; Wang, J.; Regier, T.; Dai, H. J. Co_3O_4 Nanocrystals on Graphene as a Synergistic Catalyst for Oxygen Reduction Reaction. *Nat. Mater.* **2011**, *10*, 780−786.

(10) Silva, R.; Al-Sharab, J.; Asefa, T. Edge-Plane-Rich Nitrogen-Doped Carbon Nanoneedles and Efficient Metal-Free Electrocatalysts. *Angew. Chem. Int. Ed* **2012**, *51*, 7171−7175.

(11) Pan, D.; Ombaba, M.; Zhou, Z. Y.; Liu, Y.; Chen, S. W.; Lu, J. Direct Growth of Carbon Nanofibers to Generate a 3D Porous Platform on a Metal Contact to Enable an Oxygen Reduction Reaction. *ACS Nano* **2012**, *6*, 10720−10726.

(12) Liang, Y. Y.; Wang, H. L.; Zhou, J. G.; Li, Y. G.; Wang, J.; Regier, T.; Dai, H. J. Covalent Hybrid of Spinel Manganese-Cobalt Oxide and Graphene as Advanced Oxygen Reduction Electrocatalysts. *J. Am. Chem. Soc.* **2012**, *134*, 3517−3523.

(13) Zhang, C.; Mahmood, N.; Yin, H.; Liu, F.; Hou, Y. Synthesis of Phosphorus-Doped Graphene and its Multifunctional Applications for Oxygen Reduction Reaction and Lithium Ion Batteries. *Adv. Mater.* **2013**, *25*, 4932−4937.

(14) Chen, S.; Bi, J. Y.; Zhao, Y.; Yang, L. J.; Zhang, C.; Ma, Y. W.; Wu, Q.; Wang, X. Z.; Hu, Z. Nitrogen-Doped Carbon Nanocages as Efficient Metal-Free Electrocatalysts for Oxygen Reduction Reaction. *Adv. Mater.* **2012**, *24*, 5593−5597.

(15) Lin, Z. Y.; Waller, G.; Liu, Y.; Liu, M. L.; Wong, C. P. Facile Synthesis of Nitrogen-Doped Graphene via Pyrolysis of Graphene Oxide and Urea, and its Electrocatalytic Activity toward the Oxygen-Reduction Reaction. *Adv. Energy Mater.* **2012**, *2*, 884−888.

(16) Yang, L. J.; Jiang, S. J.; Zhao, Y.; Zhu, L.; Chen, S.; Wang, X. Z.; Wu, Q.; Ma, J.; Ma, Y. W.; Hu, Z. Boron-Doped Carbon Nanotubes as Metal-Free Electrocatalysts for the Oxygen Reduction Reaction. *Angew. Chem., Int. Ed* **2011**, *50*, 7132−7135.

(17) Yang, Z.; Yao, Z.; Li, G. F.; Fang, G. Y.; Nie, H. G.; Liu, Z.; Zhou, X. M.; Chen, X.; Huang, S. M. Sulfur-Doped Graphene as an Efficient Metal-free Cathode Catalyst for Oxygen Reduction. *ACS Nano* **2012**, *6*, 205−211.

(18) Liu, Z. W.; Peng, F.; Wang, H. J.; Yu, H.; Zheng, W. X.; Yang, J. A. Phosphorus-Doped Graphite Layers with High Electrocatalytic Activity for the O_2 Reduction in an Alkaline Medium. *Angew. Chem., Int. Ed* **2011**, *50*, 3257−3261.

(19) Zhang, L.; Su, Z.; Jiang, F.; Yang, L.; Qian, J.; Zhou, Y.; Li, W.; Hong, M. Highly Graphitized Nitrogen-Doped Porous Carbon Nanopolyhedra Derived from ZIF-8 Nanocrystals as Efficient Electrocatalysts for Oxygen Reduction Reactions. *Nanoscale* **2014**, *6*, 6590−6602.

(20) Jiang, H.; Zhu, Y.; Feng, Q.; Su, Y.; Yang, X.; Li, C. Nitrogen and Phosphorus Dual-Doped Hierarchical Porous Carbon Foams as Efficient Metal-Free Electrocatalysts for Oxygen Reduction Reactions. *Chem.—Eur. J.* **2014**, *20*, 3106−3112.

(21) Ding, W.; Wei, Z.; Chen, S.; Qi, X.; Yang, T.; Hu, J.; Wang, D.; Wan, L.-J.; Alvi, S. F.; Li, L. Space-Confinement-Induced Synthesis of Pyridinic- and Pyrrolic-Nitrogen-Doped Graphene for the Catalysis of Oxygen Reduction. *Angew. Chem., Int. Ed* **2013**, *52*, 11755−11759.

(22) Wei, W.; Liang, H.; Parvez, K.; Zhuang, X.; Feng, X.; Müllen, K. Nitrogen-Doped Carbon Nanosheets with Size-Defined Mesopores as Highly Efficient Metal-Free Catalyst for the Oxygen Reduction Reaction. *Angew. Chem., Int. Ed* **2014**, *53*, 1570−1574.

(23) Phuengprasop, T.; Sittiwong, J.; Unob, F. Removal of Heavy Metal Ions by Iron Oxide Coated Sewage Sludge. *J. Hazard Mater.* **2011**, *186*, 502−507.

(24) Singh, R. P.; Agrawal, M. Variations in Heavy Metal Accumulation, Growth and Yield of Rce Plants Grown at Different Sewage Sludge Amendment Rates. *Ecotox Environ. Safe* **2010**, *73*, 632−641.

(25) Zhang, G. D.; Zhao, Q. L.; Jiao, Y.; Wang, K.; Lee, D. J.; Ren, N. Q. Efficient Electricity Generation From Sewage Sludge Using Biocathode Microbial Fuel Cell. *Water Res.* **2012**, *46*, 43−52.

(26) Xiao, B. Y.; Yang, F.; Liu, J. X. Enhancing Simultaneous Electricity Production and Reduction of Sewage Sludge in Two-Chamber MFC by Aerobic Sudge Digestion and Sludge Pretreatments. *J. Hazard Mater.* **2011**, *189*, 444−449.

(27) Wei, W. T.; Lu, Y. Z.; Chen, W.; Chen, S. W. One-Pot Synthesis, Photoluminescence, and Electrocatalytic Properties of Subnanometer-Sized Copper Clusters. *J. Am. Chem. Soc.* **2011**, *133*, 2060−2063.

(28) Deng, D. H.; Yu, L.; Chen, X. Q.; Wang, G. X.; Jin, L.; Pan, X. L.; Deng, J.; Sun, G. Q.; Bao, X. H. Iron Encapsulated within Pod-like Carbon Nanotubes for Oxygen Reduction Reaction. *Angew. Chem., Int. Ed* **2013**, *52*, 371−375.

(29) Duan, J. J.; Zheng, Y.; Chen, S.; Tang, Y. H.; Jaroniec, M.; Qiao, S. Z. Mesoporous Hybrid Material Composed of Mn_3O_4 Nanoparticles on Nitrogen-Doped Graphene for Highly Efficient Oxygen Reduction Reaction. *Chem. Commun.* **2013**, *49*, 7705−7707.

(30) Yuan, Y.; Yuan, T.; Wang, D.; Tang, J.; Zhou, S. Sewage Sludge Biochar as an Efficient Catalyst for Oxygen Reduction Reaction in an Microbial Fuel Cell. *Bioresour. Technol.* **2013**, *144*, 115−120.

(31) Wang, H.; Li, Z.; Tak, J. K.; Holt, C. M. B.; Tan, X.; Xu, Z.; Amirkhiz, B. S.; Harfield, D.; Anyia, A.; Stephenson, T.; Mitlin, D. Supercapacitors Based on Carbons with Tuned Porosity Derived from Paper Pulp Mill Sludge Biowaste. *Carbon* **2013**, *57*, 317−328.

(32) Qu, L. T.; Liu, Y.; Baek, J. B.; Dai, L. M. Nitrogen-Doped Graphene as Efficient Metal-Free Electrocatalyst for Oxygen Reduction in Fuel Cells. *ACS Nano* **2010**, *4*, 1321−1326.

(33) Bard, A. J.; Faulkner, L. R. *Electrochemical Methods: Fundamentals and Applications*, 2nd ed.; John Wiley: New York, 2001.

(34) Zhang, J. *PEM Fuel Cell Electrocatalysts and Catalyst Layers: Fundamentals and Applications*; Springer: London, 2008.

(35) Ojeda, J. J.; Romero-Gonzalez, M. E.; Bachmann, R. T.; Edyvean, R. G. J.; Banwart, S. A. Characterization of the Cell Surface and Cell Wall Chemistry of Drinking Water Bacteria by Combining XPS, FTIR Spectroscopy, Modeling, and Potentiometric Titrations. *Langmuir* **2008**, *24*, 4032−4040.

(36) Sun, H. M.; Cao, L. Y.; Lu, L. H. Bacteria Promoted Hierarchical Carbon Materials for High-Performance Supercapacitor. *Energy Environ. Sci.* **2012**, *5*, 6206−6213.